

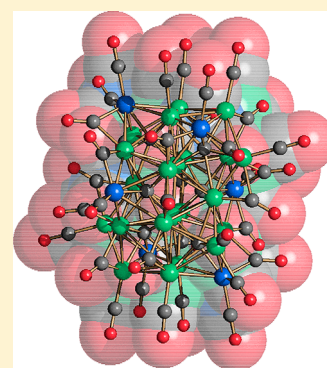
Bimetallic Nickel–Cobalt Hexacarbido Carbonyl Clusters $[\text{H}_{6-n}\text{Ni}_{22}\text{Co}_6\text{C}_6(\text{CO})_{36}]^{n-}$ ($n = 3-6$) Possessing Polyhydride Nature and Their Base-Induced Degradation to the Monoacetylide $[\text{Ni}_9\text{CoC}_2(\text{CO})_{16-x}]^{3-}$ ($x = 0, 1$)

Iacopo Ciabatti, Cristina Femoni, Maria Carmela Iapalucci, Giuliano Longoni, and Stefano Zacchini*

Dipartimento di Chimica Fisica e Inorganica, Università di Bologna, Viale Risorgimento 4, 40136 Bologna, Italy

S Supporting Information

ABSTRACT: The reaction of $[\text{Ni}_{10}\text{C}_2(\text{CO})_{16}]^{2-}$ with $\text{Co}_3(\mu_3\text{-CCl})(\text{CO})_9$ results in the new bimetallic Ni–Co hexacarbido carbonyl clusters $[\text{H}_{6-n}\text{Ni}_{22}\text{Co}_6\text{C}_6(\text{CO})_{36}]^{n-}$ ($n = 3-6$), which possess polyhydride nature and can be interconverted by means of acid–base reactions. The tetra-anion $[\text{H}_2\text{Ni}_{22}\text{Co}_6\text{C}_6(\text{CO})_{36}]^{4-}$ and the hexa-anion $[\text{Ni}_{22}\text{Co}_6\text{C}_6(\text{CO})_{36}]^{6-}$ have been isolated in a crystalline state and structurally characterized via X-ray crystallography. The six carbide atoms are lodged into Ni_7CoC square antiprismatic cages. Addition of strong bases to $[\text{Ni}_{22}\text{Co}_6\text{C}_6(\text{CO})_{36}]^{6-}$ affords mixtures of the monoacetylides $[\text{Ni}_9\text{CoC}_2(\text{CO})_{16}]^{3-}$ and $[\text{Ni}_9\text{CoC}_2(\text{CO})_{15}]^{3-}$, which have been cocrystallized as $[\text{NET}_4]_3[\text{Ni}_9\text{CoC}_2(\text{CO})_{16-x}]^{3-}$ ($x = 0.58-0.84$) salts, displaying tightly bonded interstitial C_2 units.



1. INTRODUCTION

Several bimetallic Ni–Co carbide and acetylide carbonyl clusters are known, i.e., $[\text{Co}_2\text{Ni}_{10}\text{C}(\text{CO})_{20}]^{2-}$, $[\text{Co}_3\text{Ni}_9\text{C}(\text{CO})_{20}]^{2-}$,¹ $[\text{Co}_3\text{Ni}_9\text{C}(\text{CO})_{20}]^{3-}$,² $[\text{Co}_3\text{Ni}_7\text{C}_2(\text{CO})_{15}]^{3-}$, $[\text{Co}_3\text{Ni}_7\text{C}_2(\text{CO})_{16}]^{n-}$ ($n = 2, 3$),³ and $[\text{Co}_6\text{Ni}_2\text{C}_2(\text{CO})_{16}]^{2-}$.⁴ Their highest nuclearity is 12, and the Ni/Co ratio ranges from 0.33 to 5. The wide variability of the Ni/Co composition of these clusters is due to the fact that both metals form homometallic as well as carbido carbonyl clusters, and thus, several carbonyl precursors are available for the synthesis of bimetallic Ni–Co carbides via redox condensation.⁵

Bimetallic carbonyl clusters are useful precursors for the preparation of metal nanoparticles with controlled composition.^{6–13} Thus, the possibility to prepare bimetallic Ni–Co molecular clusters with very different Ni/Co compositions makes these clusters quite attractive for the preparation of bimetallic magnetic Ni–Co nanoparticles, allowing a gradual variation of their properties. A fine control of the composition of the resulting bimetallic nanoparticles might result in a better understanding of the relationships existing between composition and properties of the nanoparticles.

In addition, bimetallic and heteronuclear clusters often display rather different properties than the analogous homometallic species and can more easily reach higher nuclearities. This point makes bimetallic carbido carbonyl clusters attractive also from a molecular point of view.^{14–18}

Thus, we started a reinvestigation of Ni–Co carbide carbonyl clusters, aiming at obtaining higher nuclearity species. Herein, we report on the study of the reaction between $[\text{Ni}_{10}\text{C}_2(\text{CO})_{16}]^{2-}$ and $\text{Co}_3(\mu_3\text{-CCl})(\text{CO})_9$, and the consequent

isolation and structural characterization of the new hexacarbides $[\text{H}_{6-n}\text{Ni}_{22}\text{Co}_6\text{C}_6(\text{CO})_{36}]^{n-}$ ($n = 3-6$), which represent more than twice an increase of the maximum nuclearity of Co–Ni–C clusters. Their reactions with strong bases, such as $[\text{NBu}_4][\text{OH}]$, besides revealing the polyhydride nature of these clusters, afforded the new monoacetylide $[\text{Ni}_9\text{CoC}_2(\text{CO})_{16-x}]^{3-}$ ($x = 0, 1$), structurally related to $[\text{Ni}_{10}\text{C}_2(\text{CO})_{16}]^{2-}$.

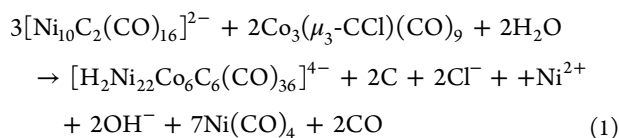
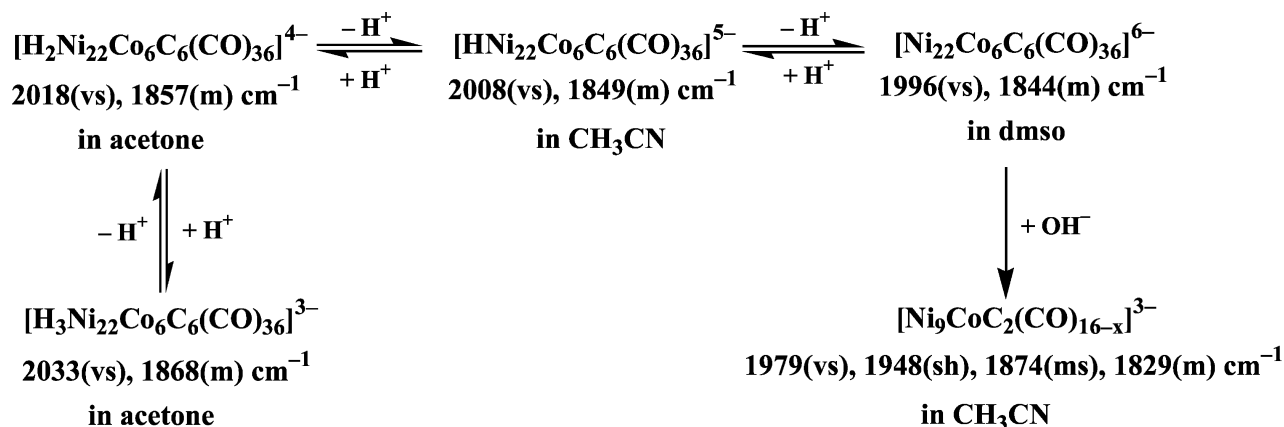
2. RESULTS AND DISCUSSION

2.1. Synthesis of $[\text{H}_{6-n}\text{Ni}_{22}\text{Co}_6\text{C}_6(\text{CO})_{36}]^{n-}$ ($n = 3-6$) and $[\text{Ni}_9\text{CoC}_2(\text{CO})_{16-x}]^{3-}$ ($x = 0, 1$). The slow addition of an acetone solution of $\text{Co}_3(\mu_3\text{-CCl})(\text{CO})_9$ to $[\text{Ni}_{10}(\text{C}_2)(\text{CO})_{16}]^{2-}$ dissolved in acetone results in the formation of a considerable amount of $\text{Ni}(\text{CO})_4$ together with a new brown species, which has been isolated after removal of the solvent *in vacuo*, washing with water and toluene, and extraction of the residue in CH_3CN . In this solvent, the new brown cluster displays $\nu(\text{CO})$ at 2008(vs) and 1849(m) cm^{-1} . After layering *n*-hexane and diisopropyl ether on the CH_3CN solution, crystals suitable for X-ray analysis of $[\text{NET}_4]_4[\text{H}_2\text{Ni}_{22}\text{Co}_6\text{C}_6(\text{CO})_{36}]^{4-}$ were obtained. The formation of $[\text{H}_2\text{Ni}_{22}\text{Co}_6\text{C}_6(\text{CO})_{36}]^{4-}$ is formally in agreement with eq 1:

Received: May 15, 2012

Published: June 12, 2012

Scheme 1



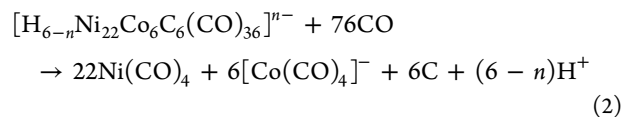
The crystals of $[\text{NEt}_4]_4[\text{H}_2\text{Ni}_{22}\text{Co}_6\text{C}_6(\text{CO})_{36}]$ are slightly soluble in thf, where they display $\nu(\text{CO})$ at 2023(vs) and 1859(m) cm^{-1} , corresponding to the dihydride tetra-anion $[\text{H}_2\text{Ni}_{22}\text{Co}_6\text{C}_6(\text{CO})_{36}]^{4-}$. The same species is completely soluble in acetone, where it displays $\nu(\text{CO})$ at 2018(vs) and 1857(m) cm^{-1} . The dihydride tetra-anion $[\text{H}_2\text{Ni}_{22}\text{Co}_6\text{C}_6(\text{CO})_{36}]^{4-}$ is deprotonated to the monohydride penta-anion $[\text{HNi}_{22}\text{Co}_6\text{C}_6(\text{CO})_{36}]^{5-}$ after dissolution in the more basic CH_3CN (Scheme 1), as shown by a significant lowering of its IR carbonyl absorptions. Thus, the penta-anion displays $\nu(\text{CO})$ at 2008(vs) and 1849(m) cm^{-1} in CH_3CN , corresponding to the species observed in solution before crystallization. Further deprotonation of $[\text{HNi}_{22}\text{Co}_6\text{C}_6(\text{CO})_{36}]^{5-}$ to yield the hexa-anion $[\text{Ni}_{22}\text{Co}_6\text{C}_6(\text{CO})_{36}]^{6-}$ occurs in CH_3CN only upon addition of solid Na_2CO_3 . Its nature and charge have been confirmed since it has been possible to isolate it as crystals of $[\text{NMe}_4]_6[\text{Ni}_{22}\text{Co}_6\text{C}_6(\text{CO})_{36}] \cdot 4\text{CH}_3\text{CN}$ by slow diffusion of *n*-hexane and di-isopropyl ether on the basified solution. The hexa-anion displays $\nu(\text{CO})$ at 1996(vs) and 1844(m) cm^{-1} in dmso and at 1988(vs) and 1824(m) cm^{-1} in Nujol mull. Conversely, addition of strong acids such as HBF_4 to an acetone solution of the dihydride tetra-anion $[\text{H}_2\text{Ni}_{22}\text{Co}_6\text{C}_6(\text{CO})_{36}]^{4-}$ results in the formation of the trihydride trianion $[\text{H}_3\text{Ni}_{22}\text{Co}_6\text{C}_6(\text{CO})_{36}]^{3-}$, which displays $\nu(\text{CO})$ at 2033(vs) and 1868(m) cm^{-1} in acetone.

The hydride nature of the $[\text{H}_{6-n}\text{Ni}_{22}\text{Co}_6\text{C}_6(\text{CO})_{36}]^{n-}$ ($n = 3-6$) anions is suggested by the observed shifts of their $\nu(\text{CO})$ bands as a function of the basicity of the solvent and/or after addition of acids or bases to their solutions in accordance with Scheme 1 and by the isolation of both the tetra- and hexa-anion. Such a suggestion is further implemented by electrochemical studies, which clearly point out that $[\text{H}_2\text{Ni}_{22}\text{Co}_6\text{C}_6(\text{CO})_{36}]^{4-}$ and $[\text{HNi}_{22}\text{Co}_6\text{C}_6(\text{CO})_{36}]^{5-}$ display different voltammetric profiles. If they were the same species in a different oxidation state, they would have, conversely, shown the same electrochemical behavior, as previously discussed.^{6,19-24} In particular, $[\text{H}_2\text{Ni}_{22}\text{Co}_6\text{C}_6(\text{CO})_{36}]^{4-}$ displays two reduction processes with features of chemical reversibility ($E_{4-/5-}^{\circ} = -0.533$ V; $E_{5-/6-}^{\circ} = -0.833$ V, in acetone), whereas $[\text{HNi}_{22}\text{Co}_6\text{C}_6(\text{CO})_{36}]^{5-}$ displays three reductions

($E_{5-/6-}^{\circ} = -0.961$ V; $E_{6-/7-}^{\circ} = -1.293$ V; $E_{7-/8-}^{\circ} = -1.666$ V, in CH_3CN). Therefore, the changes in $\nu(\text{CO})$ reported in Scheme 1 cannot be due to redox reactions. Unfortunately, all attempts to directly confirm the hydride nature of these clusters via ^1H NMR failed. We have recently discussed the problems of detecting hydrides in high-nuclearity carbonyl clusters, showing that above a nuclearity of ca. 22 all ^1H NMR resonances disappear since they become so broad as to get blurred in the baseline of the spectrum.^{6,19-25} Thus, as already reported, the hydride nature of large metal carbonyl clusters can be only indirectly inferred from joined chemical and electrochemical experiments.

The nature of the $[\text{H}_{6-n}\text{Ni}_{22}\text{Co}_6\text{C}_6(\text{CO})_{36}]^{n-}$ ($n = 3-6$) anions has been confirmed also by means of ESI-MS analyses. For example, crystals of $[\text{NEt}_4]_4[\text{H}_2\text{Ni}_{22}\text{Co}_6\text{C}_6(\text{CO})_{36}]$ dissolved in CH_3CN display ES⁻ peaks (relative intensity in parentheses) at m/z 889 (70), 880 (100), 870 (30), 862 (25), and 850 (35) attributable to stepwise CO loss from the molecular anion, i.e., $[\text{M} - 2\text{CO}]^{3-}$, $[\text{M} - 3\text{CO}]^{3-}$, $[\text{M} - 4\text{CO}]^{3-}$, $[\text{M} - 5\text{CO}]^{3-}$, and $[\text{M} - 6\text{CO}]^{3-}$, respectively. A further peak at 932 (25) is due to the adduct $\{[\text{M} - 2\text{CO}][\text{NEt}_4]\}^{3-}$. Since Ni and Co have very similar atomic masses (i.e., 58.69 and 58.93 g mol⁻¹), it is not possible to completely support the metal composition of the cluster on the basis only of ESI-MS analyses. Thus, we have analyzed different crystals via EDS coupled to a scanning electron microscope (SEM), resulting in a Ni/Co ratio of ca. 22/6.

The $[\text{H}_{6-n}\text{Ni}_{22}\text{Co}_6\text{C}_6(\text{CO})_{36}]^{n-}$ ($n = 3-6$) anions are not stable under CO atmosphere, being completely decomposed, yielding $\text{Ni}(\text{CO})_4$ and $[\text{Co}(\text{CO})_4]^-$ as the only carbonyl species detected in solution, in accordance with eq 2:



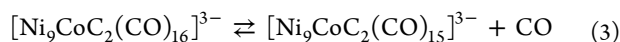
The hexa-anion $[\text{Ni}_{22}\text{Co}_6\text{C}_6(\text{CO})_{36}]^{6-}$ reacts with excess $[\text{NBu}_4][\text{OH}]$, yielding the new monoacetylide $[\text{Ni}_9\text{CoC}_2(\text{CO})_{16-x}]^{3-}$ ($x = 0, 1$). The fact that $[\text{Ni}_{22}\text{Co}_6\text{C}_6(\text{CO})_{36}]^{6-}$ is not further deprotonated can be taken as an indirect proof of the number of hydride ligands in $[\text{H}_{6-n}\text{Ni}_{22}\text{Co}_6\text{C}_6(\text{CO})_{36}]^{n-}$ ($n = 3-6$).

$[\text{Ni}_9\text{CoC}_2(\text{CO})_{16-x}]^{3-}$ ($x = 0, 1$) has been isolated in good yields after removal of the solvent *in vacuo*, washing the residue with water, thf, and acetone, and, then, extracting in CH_3CN . Crystals suitable for X-ray analyses of

[NEt₄]₃[Ni₉CoC₂(CO)_{16-x}] were obtained by slow diffusion of *n*-hexane and di-isopropyl ether on the CH₃CN solution. The Ni/Co composition has been ascertained by EDS-SEM analyses of different crystals, showing very similar results.

The fractionary index of [NEt₄]₃[Ni₉CoC₂(CO)_{16-x}] is due to the fact that, within the same crystals, mixtures of structurally related [Ni₉CoC₂(CO)₁₆]³⁻ and [Ni₉CoC₂(CO)₁₅]³⁻ clusters are present. Their ratio varies from batch to batch, probably because, depending on the experimental conditions, a different amount of CO may be lost during the synthesis. This has been confirmed by analyzing several crystals obtained from different batches. Four different CIF files are included with this paper corresponding to crystals of [NEt₄]₃[Ni₉CoC₂(CO)_{16-x}] obtained from three different reaction batches (a–c) and in particular (a) *x* = 0.84 and *x* = 0.82 (two crystals from the same batch a); (b) *x* = 0.58; and (c) 0.70. Crystals from the same batch show the same composition, as expected from the statistical crystallization of the [Ni₉CoC₂(CO)₁₆]³⁻ and [Ni₉CoC₂(CO)₁₅]³⁻ mixtures present in solution. Conversely, crystals from different batches display different compositions, indicating that the two species are formed in different ratios depending on slight variations of the experimental conditions.

[Ni₉CoC₂(CO)₁₆]³⁻ and [Ni₉CoC₂(CO)₁₅]³⁻ may be formally interchanged by reaction 3:



Nonetheless, [Ni₉CoC₂(CO)₁₆]³⁻ is stable under N₂, and even under vacuum eq 3 is not observed. Thus, the two products are likely formed in parallel during the reaction of [Ni₂₂Co₆C₆(CO)₃₆]⁶⁻ with [NBu₄][OH]. Moreover, [Ni₉CoC₂(CO)_{16-x}]³⁻ is decomposed under CO atmosphere, resulting in the formation of Ni(CO)₄ and [Co(CO)₄]⁻.

The crystals of [NEt₄]₃[Ni₉CoC₂(CO)_{16-x}] show $\nu(\text{CO})$ at 2043(w), 2005(w), 1958(vs), 1920(m), 1832(ms), and 1772(m) cm⁻¹ in Nujol mull. They are insoluble in thf, slightly soluble in acetone [$\nu(\text{CO})$ 1976(vs), 1942(sh), 1840(br) cm⁻¹] and completely soluble in CH₃CN [$\nu(\text{CO})$: 1979(vs), 1948(sh), 1874(ms), 1829(m) cm⁻¹].

2.2. Crystal Structures of [NEt₄]₄[H₂Ni₂₂Co₆C₆(CO)₃₆], [NMe₄]₆[Ni₂₂Co₆C₆(CO)₃₆]⁶⁻ · 4CH₃CN, and [NEt₄]₃[Ni₉CoC₂(CO)_{16-x}] (*x* = 0.58). The molecular structures of the tetra-anion [H₂Ni₂₂Co₆C₆(CO)₃₆]⁴⁻ and the hexa-anion [Ni₂₂Co₆C₆(CO)₃₆]⁶⁻ have been determined crystallographically on their [NEt₄]₄[H₂Ni₂₂Co₆C₆(CO)₃₆] and [NMe₄]₆[Ni₂₂Co₆C₆(CO)₃₆]⁶⁻ · 4CH₃CN salts, respectively. In both cases, only half of a cluster anion is present within the asymmetric unit of the unit cell, the whole anions being generated by an inversion center. The molecular structures of the two cluster anions are almost identical (Figure 1 and Table 1) with respect to the geometry of the metal core, the stereochemistry of the CO ligands, and all bonding distances. The cluster comprises 28 metal atoms, and the relative composition (22 Ni, 6 Co) has been independently confirmed by elemental and EDS-SEM analyses. The assignment of the positions to Ni and Co have been based on the fact that there are six similar sites displaying the lowest M–M connectivity and highest M–CO coordination, and these have been labeled as the six Co atoms. Free refinement of all positions as disordered Co/Ni confirmed the above assignment and suggests that no site disorder is present, even if X-ray crystallography is not the best way to distinguish between Ni and Co.

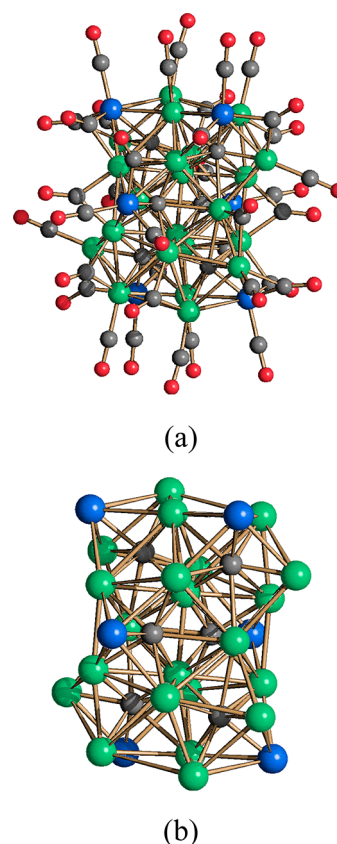


Figure 1. Molecular structure (a) and the metal framework (b) of [H_{6-n}Ni₂₂Co₆C₆(CO)₃₆]ⁿ⁻ (*n* = 4, 6) (green, Ni; blue, Co; gray, C; red, O).

Table 1. Main Bond Distances (Å) for [H_{6-n}Ni₂₂Co₆C₆(CO)₃₆]ⁿ⁻ (*n* = 4, 6)

	[H ₂ Ni ₂₂ Co ₆ C ₆ (CO) ₃₆] ⁴⁻	[Ni ₂₂ Co ₆ C ₆ (CO) ₃₆] ⁶⁻
Ni–Ni	2.330(16)–3.2680(10) average 2.613(8)	2.337(3)–3.298(5) average 2.617(2)
Ni–Ni (interstitial) ^a	2.330(16)	2.337(3)
Ni–Co	2.4283(11)–2.6315(11) average 2.524(4)	2.398(3)–2.652(3) average 2.525(9)
Ni–C	1.881(6)–2.328(6) average 2.08(3)	1.911(12)–2.368(13) average 2.09(5)
Co–C	1.925(6)–1.968(6) average 1.952(15)	1.858(13)–1.910(14) average 1.892(19)

^aThis refers to the two fully interstitial Ni atoms.

The metal core of the [H_{6-n}Ni₂₂Co₆C₆(CO)₃₆]ⁿ⁻ (*n* = 4, 6) clusters is rather complex and formally results from the condensation of six Ni₇CoC distorted square antiprismatic C-centered cages. Two of these Ni₇CoC polyhedra are so highly distorted that the two Ni atoms along the diagonal on one of the square faces are at bonding distance 3.03–3.05 Å, and therefore, they may be alternatively described as two Ni₅CoC trigonal prisms capped by two further Ni atoms. In all cases, each interstitial carbide atom is octa-coordinated, with rather spread Ni–C contacts [range 1.881(6)–2.328(6) Å, average 2.08(3) Å for *n* = 4; range 1.911(12)–2.368(13) Å, average 2.09(5) Å for *n* = 6], whereas the Co–C distances are distributed in a narrower range [range 1.925(6)–1.968(6) Å, average 1.952(15) Å for *n* = 4; range 1.858(13)–1.910(14) Å, average 1.892(19) Å for *n* = 6]. For comparison, the sum of the covalent radii is 1.92 Å for Ni–C and 1.94 Å for Co–C.²⁶

The $\text{Ni}_{22}\text{Co}_6$ metal core of the cluster presents 83 M–M contacts that can be considered within bonding distances: 59 Ni–Ni [range 2.330(16)–3.2680(10) Å, average 2.613(8) Å for $n = 4$; range 2.337(3)–3.298(5) Å, average 2.617(2) Å for $n = 6$] and 24 Co–Ni [range 2.4283(11)–2.6315(11) Å, average 2.524(4) Å for $n = 4$; range 2.398(3)–2.652(3) Å, average 2.525(9) Å for $n = 6$].

The average M–M connectivity is 5.93, resulting from very different situations. Thus, the six Co atoms display the lowest number of M–M bonds, i.e., 4, plus one Co–C(carbide) bond. Conversely, there are two fully interstitial Ni atoms (non-bonded to any CO) that display nine Ni–M bonding contacts and four Ni–C(carbide) bonds. It must be remarked that these two fully interstitial Ni atoms are tightly bonded together, showing the shortest Ni–Ni contact [2.330(16) Å for $n = 4$; 2.337(3) Å for $n = 6$]. The remaining 20 Ni atoms display intermediate situations. A M–M connectivity of nine is close to that found in bulk close-packed metals (12) and similar to body-centered cubic (8), suggesting (at least morphologically) metalization of these two atoms. Conversely, the situation for Co (4 M–M bonds) is similar to that found in lower nuclearity molecular clusters (e.g., $\text{Co}_6(\text{CO})_{16}$).²⁷

The surface of the cluster is completed by 36 CO ligands, 16 terminal and 20 edge bridging. The CO/M ratio is 1.286, which, by considering the two interstitial Ni atoms, corresponds to a surface coverage $\text{CO}/M_{\text{surface}}$ of 1.385. The six Co atoms display the highest number of CO ligands, one terminal and two edge bridging. This is a further (indirect) confirmation of our assignment of these sites as Co. Moreover, the addition of a further CO ligand formally results in the formation of $[\text{Co}(\text{CO})_4]^-$, suggesting a possible pathway for the CO-induced decomposition of the cluster.

The $[\text{H}_{6-n}\text{Ni}_{22}\text{Co}_6\text{C}_6(\text{CO})_{36}]^{n-}$ ($n = 3-6$) clusters possess 376 cluster valence electrons (CVE) corresponding to 188 ($6N + 20$; $N =$ number of metal atoms) cluster valence orbitals (CVO). This electron count is in keeping with other Ni polycarbide clusters, which are usually electron rich, i.e., $[\text{Ni}_{32}\text{C}_6(\text{CO})_{36}]^{6-}$ and $[\text{Ni}_{38}\text{C}_6(\text{CO})_{42}]^{6-}$ ($6N + 19$ CVO),²⁸ $[\text{Ni}_{36}\text{C}_8(\text{CO})_{36}(\text{Cd}_2\text{Cl}_3)]^{5-}$ ($6N + 19$ CVO), and $[\text{Ni}_{42}\text{C}_8(\text{CO})_{44}(\text{CdCl})]^{7-}$ ($6N + 22$ CVO).²⁴

The electronic properties of $[\text{Ni}_{22}\text{Co}_6\text{C}_6(\text{CO})_{36}]^{6-}$ have been investigated by means of extended Hückel molecular orbital (EHMO) analysis, using the program CACAO²⁹ with its crystallographic coordinates. The frontier regions (in the -11 to -9 eV interval of energy) of the EHMO diagrams of $[\text{Ni}_{22}\text{Co}_6\text{C}_6(\text{CO})_{36}]^{6-}$ are represented in Figure 2.

The diagram shows the presence of four closely spaced molecular orbitals (MOs 231–234) in an otherwise wide gap ($\Delta\text{MO}(230-235) = 0.676$ eV). The HOMO (MO 233)–LUMO (MO 232) gap is, thus, very small (0.114 eV), and the LUMO (MO 232) and LUMO+1 (MO 231) are almost degenerate (0.048 eV). The small HOMO–LUMO gap and the presence of a very low energy LUMO+1 explain the propensity of these clusters toward reduction, as indicated by electrochemical studies (see Section 2.1).

The molecular structure of the $[\text{Ni}_9\text{CoC}_2(\text{CO})_{16-x}]^{3-}$ ($x = 0, 1$) trianion has been determined in its $[\text{NET}_4]_3[\text{Ni}_9\text{CoC}_2(\text{CO})_{16-x}]$ salt (Figure 3 and Table 2). As described in the previous section, four crystals showing different values of the index x (0.58, 0.70, 0.84, 0.82) have been analyzed in order to shed some light on the composition of this cluster. A mixture of the two $[\text{Ni}_9\text{CoC}_2(\text{CO})_{16}]^{3-}$ and $[\text{Ni}_9\text{CoC}_2(\text{CO})_{15}]^{3-}$ trianions, which differ only for the number

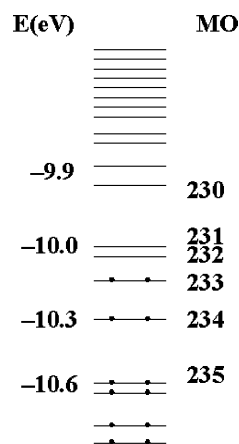


Figure 2. Frontier region (in the -11 to -9 eV interval of energy) of the EHMO diagram of $[\text{Ni}_{22}\text{Co}_6\text{C}_6(\text{CO})_{36}]^{6-}$.

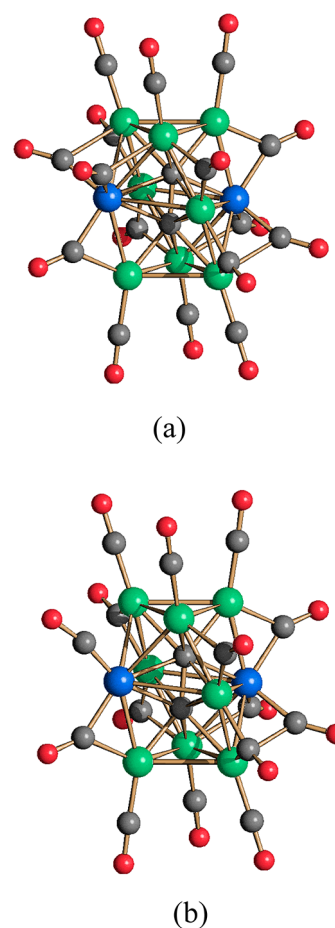


Figure 3. Molecular structure of (a) $[\text{Ni}_9\text{CoC}_2(\text{CO})_{16}]^{3-}$ and (b) $[\text{Ni}_9\text{CoC}_2(\text{CO})_{15}]^{3-}$ (green, Ni; blue, Ni/Co; gray, C; red, O).

Table 2. Main Bond Distances (Å) for $[\text{Ni}_9\text{CoC}_2(\text{CO})_{16-x}]^{3-}$ ($x = 0, 1$)^a

M–M	2.3393(8)–2.8029(9) average 2.5957(18)
M–C	1.927(6)–2.159(6) average 2.078(13)
C–C	1.455(12)

^aM denotes Ni and Co.

of CO ligands, is present within each crystal. Crystals from the same reaction batch display almost identical compositions (e.g., $x = 0.84$ and 0.82 for the two crystal data herein included as an example). Conversely, the ratio of the two clusters slightly varies from batch to batch. For instance, $[\text{NEt}_4]_3[\text{Ni}_9\text{CoC}_2(\text{CO})_{16-x}]$ ($x = 0.58$) contains 42% $[\text{Ni}_9\text{CoC}_2(\text{CO})_{16}]^{3-}$ and 58% $[\text{Ni}_9\text{CoC}_2(\text{CO})_{15}]^{3-}$, whereas $[\text{NEt}_4]_3[\text{Ni}_9\text{CoC}_2(\text{CO})_{16-x}]$ ($x = 0.70$) is composed of 30% $[\text{Ni}_9\text{CoC}_2(\text{CO})_{16}]^{3-}$ and 70% $[\text{Ni}_9\text{CoC}_2(\text{CO})_{15}]^{3-}$. This indicates that the two species are formed together within the same reaction (see Section 2.1) and their exact ratio is affected by minor variations of the experimental conditions. For simplicity, only the data of $[\text{NEt}_4]_3[\text{Ni}_9\text{CoC}_2(\text{CO})_{16-x}]$ ($x = 0.58$) will be used in the following discussion, whereas the other CIF files are included as Supporting Information.

Within the crystal, the two different trianions are generated by the fact that two edge-bridging CO ligands related by a mirror plane and bonded to a common atom are partially vacant and replaced by a single terminal CO bonded to the same metal atom. The metal composition of the crystals has been determined by means of EDS coupled to a SEM, indicating the presence of nine Ni and one Co. Even if Ni and Co are not well distinguished by X-ray crystallography, the single Co atom has been assigned as disordered over two symmetry-related positions (see Experimental Section) in the central square of the cluster. Indeed, also the above-mentioned disordered bridging-terminal CO ligands are bonded to these atoms.

The $[\text{Ni}_9\text{CoC}_2(\text{CO})_{16-x}]^{3-}$ ($x = 0, 1$) trianions are closely related to the previously reported $[\text{Ni}_{10}\text{C}_2(\text{CO})_{16}]^{2-}$,³⁰ $[\text{Co}_3\text{Ni}_7\text{C}_2(\text{CO})_{15}]^{3-}$, and $[\text{Co}_3\text{Ni}_7\text{C}_2(\text{CO})_{16}]^{n-}$ ($n = 2, 3$).³ Their common metal polyhedron may be seen as being derived from the condensation of two (distorted) capped trigonal prisms sharing a common square face. Overall, the metal framework consists of a 3,4,3 stack of metal atoms of C_{2h} idealized symmetry. The interstitial C atoms are lodged within monocapped trigonal prismatic cavities, showing seven M–C contacts each. As a result of the fact that these two M₇C prisms share a common square face, the interstitial C atoms display a very short C–C distance [1.455(12) Å], suggesting the presence of tightly bonded C₂ units. For what concerns the stereochemistry of the CO ligands, $[\text{Ni}_9\text{CoC}_2(\text{CO})_{16}]^{3-}$ contains six terminal and 10 edge-bridging carbonyls, whereas $[\text{Ni}_9\text{CoC}_2(\text{CO})_{15}]^{3-}$ possesses seven terminal and eight edge-bridging ligands.

EHMO calculations with CACAO²⁹ (Figure 4) show that $[\text{Ni}_9\text{CoC}_2(\text{CO})_{15}]^{3-}$ displays a rather wide HOMO–LUMO gap (1.416 eV) and possesses a closed-shell electronic configuration. The addition of a further CO in $[\text{Ni}_9\text{CoC}_2(\text{CO})_{16}]^{3-}$ introduces an additional MO within this gap, reducing the HOMO–LUMO gap to 0.88 eV. The latter is isoelectronic with $[\text{Ni}_{10}\text{C}_2(\text{CO})_{16}]^{2-}$,³⁰ possessing 142 CVE ($6N + 11$ CVO). Conversely, $[\text{Ni}_9\text{CoC}_2(\text{CO})_{15}]^{3-}$ contains 140 CVE ($6N + 10$ CVO), being isoelectronic to $[\text{Co}_3\text{Ni}_7\text{C}_2(\text{CO})_{16}]^{3-}$.³ Finally, the previously reported $[\text{Co}_3\text{Ni}_7\text{C}_2(\text{CO})_{15}]^{3-}$ displays only 138 CVE ($6N + 9$ CVO) even if the metal cages are very similar. The different electron count of these decanuclear monoacetylide clusters possessing similar metal frameworks is probably due to distortions and loosening of the metal interactions.

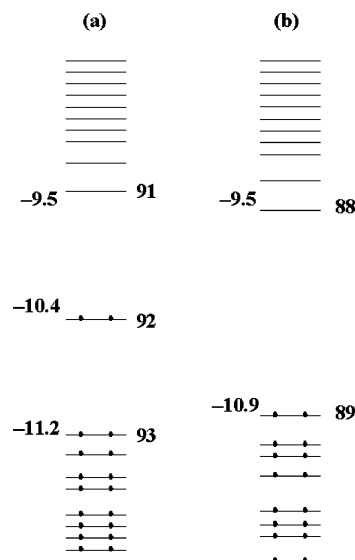


Figure 4. Frontier region (in the -12 to -8.5 eV interval of energy) of the EHMO diagrams of (a) $[\text{Ni}_9\text{CoC}_2(\text{CO})_{16}]^{3-}$ and (b) $[\text{Ni}_9\text{CoC}_2(\text{CO})_{15}]^{3-}$.

3. CONCLUSIONS

The new bimetallic Ni–Co hexacarbido carbonyl clusters $[\text{H}_{6-n}\text{Ni}_{22}\text{Co}_6\text{C}_6(\text{CO})_{36}]^{n-}$ ($n = 3–6$) have been prepared, and the tetra- and hexa-anions structurally characterized. These results confirm the capability of interstitial heteroatoms, among which are carbides, to stabilize larger metal carbonyl clusters.^{16,31,32} Moreover, this enhanced stability contributes also to the development of peculiar physical properties, such as multivalence.^{6,14} Thus, the $[\text{H}_{6-n}\text{Ni}_{22}\text{Co}_6\text{C}_6(\text{CO})_{36}]^{n-}$ ($n = 4, 5$) anions display some redox processes that are reversible under electrochemical control. These redox properties are in keeping with the EHMO diagrams, which display a very small HOMO–LUMO gap and the presence of several MOs in the frontier region with rather similar energies.

In addition, joined electrochemical and chemical experiments result as being the only tools available to elucidate the polyhydride nature of such large carbonyl clusters, since their hydride atoms are ¹H NMR silent. This point has already been discussed in the literature, even if a satisfactory explanation of this phenomenon is still missing.^{6,19–25}

The $[\text{Ni}_{22}\text{Co}_6\text{C}_6(\text{CO})_{36}]^{6-}$ hexa-anion is degraded to $[\text{Ni}_9\text{CoC}_2(\text{CO})_{16-x}]^{3-}$ ($x = 0, 1$) after treatment with an excess of a strong base, indirectly confirming the number of hydride atoms in the parent cluster. $[\text{Ni}_9\text{CoC}_2(\text{CO})_{16-x}]^{3-}$ ($x = 0, 1$) is structurally related to the previously reported $[\text{Ni}_{10}\text{C}_2(\text{CO})_{16}]^{2-}$,³⁰ $[\text{Co}_3\text{Ni}_7\text{C}_2(\text{CO})_{15}]^{3-}$, and $[\text{Co}_3\text{Ni}_7\text{C}_2(\text{CO})_{16}]^{n-}$ ($n = 2, 3$).³ They are all based on the condensation of two distorted monocapped C-centered trigonal prisms sharing a common square face, which allows the formation of a direct C–C bond. Nonetheless, their electron counts range from $6N + 9$ CVO for $[\text{Co}_3\text{Ni}_7\text{C}_2(\text{CO})_{15}]^{3-}$ to $6N + 10$ for $[\text{Co}_3\text{Ni}_7\text{C}_2(\text{CO})_{16}]^{3-}$ as well as $[\text{Ni}_9\text{CoC}_2(\text{CO})_{15}]^{3-}$ and, eventually, $6N + 11$ in the cases of $[\text{Ni}_{10}\text{C}_2(\text{CO})_{16}]^{2-}$ and $[\text{Ni}_9\text{CoC}_2(\text{CO})_{16}]^{3-}$. This results in deformations of their metal cages and loosening of some M–M bonds, even though the overall structures are rather similar. Thus, even for relatively small clusters such as these decanuclear species, the assignment of their structures based

Table 3. Crystal Data and Experimental Details for [NEt₄]₄[H₂Ni₂₂Co₆C₆(CO)₃₆], [NMe₄]₆[Ni₂₂Co₆C₆(CO)₃₆] \cdot 4CH₃CN, and [NEt₄]₃[Ni₉CoC₂(CO)_{16-x}] (x = 0.58)

	[NEt ₄] ₄ [H ₂ Ni ₂₂ Co ₆ C ₆ (CO) ₃₆]	[NMe ₄] ₆ [Ni ₂₂ Co ₆ C ₆ (CO) ₃₆] \cdot 4CH ₃ CN	[NEt ₄] ₃ [Ni ₉ CoC ₂ (CO) _{16-x}] (x = 0.58)
formula	C ₇₄ H ₈₀ Co ₆ N ₄ Ni ₂₂ O ₃₆	C ₇₄ H ₈₄ Co ₆ N ₁₀ Ni ₂₂ O ₃₆	C _{41.42} H ₆₀ Co ₃ Ni ₉ O _{15.42}
fw	3246.62	3334.71	1434.00
T, K	100(2)	100(2)	293(2)
λ , Å	0.71073	0.71073	0.71073
cryst syst	orthorhombic	triclinic	orthorhombic
space group	<i>Pbca</i>	<i>P</i> $\bar{1}$	<i>Pnmm</i>
<i>a</i> , Å	18.233(2)	14.578(3)	12.0473(12)
<i>b</i> , Å	21.495(3)	14.582(3)	12.2173(12)
<i>c</i> , Å	24.119(3)	15.213(4)	18.4801(18)
α , deg	90	62.964(3)	90
β , deg	90	63.929(3)	90
γ , deg	90	87.386(3)	90
cell volume, Å ³	9453(2)	2539.1(10)	2720.0(5)
Z	4	1	2
<i>D</i> _c , g cm ⁻³	2.281	2.181	1.751
μ , mm ⁻¹	5.364	4.997	3.398
<i>F</i> (000)	6472	1664	1464
cryst size, mm	0.21 \times 0.16 \times 0.12	0.18 \times 0.15 \times 0.12	0.21 \times 0.16 \times 0.12
θ limits, deg	1.69–26.00	1.58–25.03	2.00–25.55
index ranges	–22 $\leq h \leq$ 22 –26 $\leq k \leq$ 26 –29 $\leq l \leq$ 29	–17 $\leq h \leq$ 17 –17 $\leq k \leq$ 17 –18 $\leq l \leq$ 18	–14 $\leq h \leq$ 14 –14 $\leq k \leq$ 14 –22 $\leq l \leq$ 22
reflns collected	93 522	23 617	25 873
indep reflns	9285 [<i>R</i> _{int} = 0.0924]	8910 [<i>R</i> _{int} = 0.0574]	2637 [<i>R</i> _{int} = 0.0351]
completeness to θ max	100.0%	99.3%	99.9%
data/restraints/params	9285/0/640	8910/253/623	2637/205/278
goodness on fit on <i>F</i> ²	1.075	1.061	1.225
<i>R</i> ₁ (<i>I</i> > 2 σ (<i>I</i>))	0.0420	0.0885	0.0407
<i>wR</i> ₂ (all data)	0.1171	0.2653	0.1027
largest diff. peak and hole, e Å ⁻³	1.154/–0.912	2.002/–1.194	0.559/–0.432

solely on their electron count might be taken always with some care.

Finally, this work further confirms the capacity of carbide atoms in Ni, Co, and Ni–Co carbonyl clusters to be lodged in rather different cavities such as square antiprismatic, trigonal prismatic, monocapped trigonal prismatic, and octahedral, as well as to form tightly bonded C₂ units.^{1–4,19,20,23,24,28,30,33,34} Also, the greater stabilizing effect of isolated interstitially located carbide atoms with respect to C₂ moieties^{23,34} enables obtaining higher nuclearity molecular clusters and approaching the nanosize regime. Thus, the bimetallic [H_{6-n}Ni₂₂Co₆C₆(CO)₃₆]ⁿ⁻ (*n* = 3–6) cluster displays a diameter (measured at the outer Co atoms) of ca. 0.9 nm, and the whole molecular ion has a diameter of ca. 1.5 nm once measured from the outer oxygen atoms.

4. EXPERIMENTAL SECTION

4.1. General Procedures. All reactions and sample manipulations were carried out using standard Schlenk techniques under nitrogen and in dried solvents. All the reagents were commercial products (Aldrich) of the highest purity available and used as received, except [NR₄]₂[Ni₁₀(C₂)(CO)₁₆] (R = Me, Et)³⁰ and Co₃(μ_3 -CCl)(CO)₉,³⁵ which have been prepared according to the literature. Analysis of Ni and Co were performed by atomic absorption on a Pye-Unicam instrument. The content of Ni and Co on single crystals was determined using an EVO 50 EP (ZEISS) scanning electron microscope with an Oxford INCA 350 EDS. Analyses of C, H, and N were obtained with a ThermoQuest FlashEA 1112NC instrument. IR spectra were recorded on a Perkin-Elmer SpectrumOne

interferometer in CaF₂ cells. ESI mass spectra were recorded on a Waters Micromass ZQ4000 instrument. The electrochemical experiments were performed with a PGSTAT302N (Autolab) potentiostat equipped with a nitrogen-purged three-electrode cell containing a platinum working electrode, a saturated calomel electrode (SCE) as the reference, and a Pt wire as the counter electrode; [NBu₄][BF₄] (0.1 M) was used as supporting electrolyte. Structure drawings have been performed with SCHAKAL99.³⁶

4.2. Synthesis of [NEt₄]₄[H₂Ni₂₂Co₆C₆(CO)₃₆]. A solution of Co₃(μ_3 -CCl)(CO)₉ (0.224 g, 0.471 mmol) in acetone (15 mL) was added dropwise to a solution of [NEt₄]₂[Ni₁₀(C₂)(CO)₁₆] (1.05 g, 0.818 mmol) in acetone (25 mL). An evolution of gas was immediately observed, and the solution was further stirred under nitrogen for 2 h. Then, the solvent was removed *in vacuo*, and the solid was washed with water (40 mL) and toluene (40 mL) and extracted in CH₃CN (20 mL). Crystals of [NEt₄]₄[H₂Ni₂₂Co₆C₆(CO)₃₆] suitable for X-ray analyses were obtained by slow diffusion of *n*-hexane (5 mL) and di-isopropyl ether (40 mL) (yield 0.62 g, 52% based on Ni, 82% based on Co).

Anal. Calcd for C₇₄H₈₀Co₆N₄Ni₂₂O₃₆ (3228.63): C 27.50, H 2.50, N 1.73, Co 10.95, Ni 39.48. Found: C 27.68, H 2.50, N 1.59, Co 11.12, Ni 39.64. IR (thf, 293 K) ν (CO): 2023(s), 1859(m) cm⁻¹. IR (acetone, 293 K) ν (CO): 2018(vs), 1857(m) cm⁻¹.

4.3. Synthesis of [NMe₄]₆[Ni₂₂Co₆C₆(CO)₃₆] \cdot 4CH₃CN. A solution of Co₃(μ_3 -CCl)(CO)₉ (0.224 g, 0.471 mmol) in acetone (15 mL) was added dropwise to a solution of [NMe₄]₂[Ni₁₀(C₂)(CO)₁₆] (0.958 g, 0.818 mmol) in acetone (25 mL). An evolution of gas was immediately observed, and the solution was further stirred under nitrogen for 2 h. Then, the solvent was removed *in vacuo*, and the solid was washed with water (40 mL) and toluene (40 mL) and extracted in CH₃CN (20 mL). Solid Na₂CO₃ was added and the solution stirred

overnight at room temperature. The solid was, then, removed by filtration, and crystals of $[\text{NMe}_4]_6[\text{Ni}_{22}\text{Co}_6\text{C}_6(\text{CO})_{36}] \cdot 4\text{CH}_3\text{CN}$ suitable for X-ray analyses were obtained by slow diffusion of *n*-hexane (5 mL) and di-isopropyl ether (40 mL) (yield 0.68 g, 55% based on Ni, 87% based on Co).

Anal. Calcd for $\text{C}_{74}\text{H}_{84}\text{Co}_6\text{Ni}_{22}\text{O}_{36}$ (3316.68): C 27.77, H 2.55, N 4.22, Co 10.66, Ni 38.43. Found: C 27.52, H 2.71, N 4.07, Co 10.87, Ni 38.61. IR (dmsol, 293 K) $\nu(\text{CO})$: 1996(vs), 1844(m) cm^{-1} . IR (Nujol, 293 K) $\nu(\text{CO})$: 1988(vs), 1824(m) cm^{-1} .

(a) **4.4. Deprotonation/Protonation Studies of $[\text{H}_{6-n}\text{Ni}_{22}\text{Co}_6\text{C}_6(\text{CO})_{36}]^{n-}$ ($n = 3-6$).** The tetra-anion $[\text{H}_2\text{Ni}_{22}\text{Co}_6\text{C}_6(\text{CO})_{36}]^{4-}$ [$\nu(\text{CO})$ 2018(vs), 1857(m) cm^{-1} in acetone] is protonated to the trianion $[\text{H}_3\text{Ni}_{22}\text{Co}_6\text{C}_6(\text{CO})_{36}]^{3-}$ [$\nu(\text{CO})$ 2033(vs), 1868(m) cm^{-1} in acetone] after addition of $\text{HBF}_4 \cdot \text{Et}_2\text{O}$ in acetone. In detail, $\text{HBF}_4 \cdot \text{Et}_2\text{O}$ (42.5 μL , 0.310 mmol) was added dropwise with a micropipet to a solution of $[\text{NEt}_4]_4[\text{H}_2\text{Ni}_{22}\text{Co}_6\text{C}_6(\text{CO})_{36}]$ (0.868 g, 0.269 mmol) in acetone (20 mL). The reaction was monitored by IR after each addition up to complete conversion.

(b) The tetra-anion $[\text{H}_2\text{Ni}_{22}\text{Co}_6\text{C}_6(\text{CO})_{36}]^{4-}$ [$\nu(\text{CO})$ 2018(vs), 1857(m) cm^{-1} in acetone] was deprotonated to the penta-anion $[\text{HNi}_{22}\text{Co}_6\text{C}_6(\text{CO})_{36}]^{5-}$ [$\nu(\text{CO})$ 2008(vs), 1849(m) cm^{-1} in CH_3CN] by simple dissolution in CH_3CN .

(c) The hexa-anion $[\text{Ni}_{22}\text{Co}_6\text{C}_6(\text{CO})_{36}]^{6-}$ [$\nu(\text{CO})$ 1996(vs), 1844(m) cm^{-1} in dmsol] was obtained by deprotonation of the penta-anion $[\text{HNi}_{22}\text{Co}_6\text{C}_6(\text{CO})_{36}]^{5-}$ [$\nu(\text{CO})$ 2008(vs), 1849(m) cm^{-1} in CH_3CN] after treatment in CH_3CN with Na_2CO_3 as described in Section 4.4. Alternatively, it may be obtained by treating the penta-anion $[\text{HNi}_{22}\text{Co}_6\text{C}_6(\text{CO})_{36}]^{5-}$ in CH_3CN with $[\text{NBu}_4][\text{OH}]$. In this case, the hydroxide must be added very slowly, monitoring by IR the reaction after each addition, in order to avoid formation of $[\text{Ni}_9\text{CoC}_2(\text{CO})_{16-x}]^{3-}$ as described in Section 4.5.

4.5. Synthesis of $[\text{NEt}_4]_3[\text{Ni}_9\text{CoC}_2(\text{CO})_{16-x}]$ ($x = 0.58$). A solution of $[\text{NBu}_4][\text{OH}]$ (0.348 g, 1.34 mmol) in CH_3CN (15 mL) was added dropwise to a solution of $[\text{NEt}_4]_4[\text{H}_2\text{Ni}_{22}\text{Co}_6\text{C}_6(\text{CO})_{36}]$ (0.868 g, 0.269 mmol) in CH_3CN (20 mL) over a period of 3 h. Then, the solvent was removed *in vacuo*, and the solid was washed with water (40 mL), *thf* (20 mL), and acetone (20 mL) and extracted in CH_3CN (20 mL). Crystals of $[\text{NEt}_4]_3[\text{Ni}_9\text{CoC}_2(\text{CO})_{16-x}]$ ($x = 0.58$) suitable for X-ray analyses were obtained by slow diffusion of *n*-hexane (5 mL) and di-isopropyl ether (40 mL) (yield 0.59 g, 63% based on Ni, 25% based on Co).

The value of x varies from batch to batch. The CIF files of other three crystals obtained from different reaction batches are included to support this point. They show $x = 0.70, 0.84$, and 0.82 .

Anal. Calcd for $\text{C}_{41.42}\text{H}_{60}\text{Co}_3\text{Ni}_9\text{O}_{15.42}$ (1434.00): C 34.70, H 4.22, N 2.93, Co 4.11, Ni 36.74. Found: C 34.55, H 4.40, N 2.78, Co 4.02, Ni 36.85. IR (Nujol, 293 K) $\nu(\text{CO})$: 2043(w), 2005(w), 1958(vs), 1920(m), 1832(ms), 1772(m) cm^{-1} . IR (acetone, 293 K) $\nu(\text{CO})$: 1976(vs), 1942(sh), 1840(br) cm^{-1} . IR (CH_3CN , 293 K) $\nu(\text{CO})$: 1979(vs), 1948(sh), 1874(ms), 1829(m) cm^{-1} .

4.6. X-ray Crystallographic Study. Crystal data and collection details for $[\text{NEt}_4]_4[\text{H}_2\text{Ni}_{22}\text{Co}_6\text{C}_6(\text{CO})_{36}]$, $[\text{NMe}_4]_6[\text{Ni}_{22}\text{Co}_6\text{C}_6(\text{CO})_{36}] \cdot 4\text{CH}_3\text{CN}$, and $[\text{NEt}_4]_3[\text{Ni}_9\text{CoC}_2(\text{CO})_{16-x}]$ ($x = 0.58$) are reported in Table 3. The diffraction experiments were carried out on a Bruker APEX II diffractometer equipped with a CCD detector using $\text{Mo K}\alpha$ radiation. Data were corrected for Lorentz polarization and absorption effects (empirical absorption correction SADABS).³⁷ Structures were solved by direct methods and refined by full-matrix least-squares based on all data using F^2 .³⁸ Hydrogen atoms were fixed at calculated positions and refined by a riding model. All non-hydrogen atoms were refined with anisotropic displacement parameters, unless otherwise stated.

$[\text{NEt}_4]_4[\text{H}_2\text{Ni}_{22}\text{Co}_6\text{C}_6(\text{CO})_{36}]$. The asymmetric unit of the unit cell contains half of a cluster anion (located on an inversion center) and two $[\text{NEt}_4]^+$ cations (both located on general positions).

$[\text{NMe}_4]_6[\text{Ni}_{22}\text{Co}_6\text{C}_6(\text{CO})_{36}] \cdot 4\text{CH}_3\text{CN}$. The asymmetric unit of the unit cell contains half of a cluster anion (located on an inversion

center), three $[\text{NMe}_4]^+$ cations, and two CH_3CN molecules (located on general positions). Two carbonyl ligands in the anion are disordered, and therefore they have been split into two positions each and refined isotropically using one occupancy parameter per disordered group. Similar U restraints (su 0.005) were applied to the C and O atoms. The geometries of the $[\text{NMe}_4]^+$ cations and the CH_3CN molecules were restrained to be similar (SAME line in SHELXL; su 0.02). Restraints to bond distances were applied as follow (su 0.01): 1.47 Å for C–C and 1.14 Å for C–N in CH_3CN .

$[\text{NEt}_4]_3[\text{Ni}_9\text{CoC}_2(\text{CO})_{16-x}]$ ($x = 0.58$). The structure of $[\text{NEt}_4]_3[\text{Ni}_9\text{CoC}_2(\text{CO})_{16-x}]$ has been determined on four isomorphous crystals obtained from three different reaction batches, showing different values of x (0.58, 0.70, 0.84, 0.82). The asymmetric unit of the unit cell contains one fourth of a cluster anion (located on 2/m) and one-half (located on 2) and one fourth (located on 2/m) of a $[\text{NEt}_4]^+$ cation. The half $[\text{NEt}_4]^+$ cation located on 2 is disordered over two independent positions, which have been refined anisotropically using one occupancy parameter per disordered group. Conversely, the $[\text{NEt}_4]^+$ cation located on 2/m (present as one fourth in the asymmetric unit) is disordered over four symmetry-related positions and has been refined anisotropically using a 0.25 occupancy factor. The M(2) position of the cluster anion has been assigned as disordered Ni/Co. Since this position is repeated twice on the same anion by symmetry and on the basis of EDS analyses, which indicate the presence of a single Co atom within the cluster, this position has been assigned 50% to Ni and 50% to Co. The CO ligand bonded to M(2) is disordered over two positions, one in general position and one on a mirror plane. Thus, the disordered CO has been split into two positions and refined anisotropically using one occupancy parameter per disordered group. Because of symmetry, this disorder originates two different anions, one containing 16 and the other 15 CO ligands. Similar U restraints (su 0.005) were applied to the C and O atoms. The geometries of the $[\text{NEt}_4]^+$ cations were restrained to be similar (SAME line in SHELXL; su 0.02). Restraints to bond distances were applied as follow (su 0.01): 1.53 Å for C–C and 1.47 Å for C–N in $[\text{NEt}_4]^+$.

■ ASSOCIATED CONTENT

Supporting Information

CIF files giving X-ray crystallographic data for the structure determinations of $[\text{NEt}_4]_4[\text{H}_2\text{Ni}_{22}\text{Co}_6\text{C}_6(\text{CO})_{36}]$, $[\text{NMe}_4]_6[\text{Ni}_{22}\text{Co}_6\text{C}_6(\text{CO})_{36}] \cdot 4\text{CH}_3\text{CN}$, and $[\text{NEt}_4]_3[\text{Ni}_9\text{CoC}_2(\text{CO})_{16-x}]$ ($x = 0.58, 0.70, 0.82, 0.84$). This material is available free of charge via the Internet at <http://pubs.acs.org>.

■ AUTHOR INFORMATION

Corresponding Author

*Fax: +39 0512093690. E-mail: stefano.zacchini@unibo.it

Notes

The authors declare no competing financial interest.

■ ACKNOWLEDGMENTS

The financial support of MIUR (PRIN2008) and the University of Bologna is gratefully acknowledged. Funding by Fondazione CARIPOLO, Project No. 2011-0289, is heartily acknowledged.

■ REFERENCES

- (1) Ceriotti, A.; Della Pergola, R.; Longoni, G.; Manassero, M.; Masciocchi, N.; Sansoni, M. *J. Organomet. Chem.* **1987**, *330*, 237.
- (2) Ceriotti, A.; Della Pergola, R.; Longoni, G.; Manassero, M.; Sansoni, M. *J. Chem. Soc., Dalton Trans.* **1984**, 1181.
- (3) (a) Arrigoni, A.; Ceriotti, A.; Della Pergola, R.; Longoni, G.; Manassero, M.; Sansoni, M. *J. Organomet. Chem.* **1985**, *296*, 243. (b) Longoni, G.; Ceriotti, A.; Della Pergola, R.; Manassero, M.;

Perego, M.; Piro, G.; Sansoni, M. *Philos. Trans. R. Soc. London A* **1982**, 308, 47.

(4) Arrigoni, A.; Ceriotti, A.; Della Pergola, R.; Manassero, M.; Masciocchi, N.; Sansoni, M. *Angew. Chem., Int. Ed. Engl.* **1984**, 23, 322.

(5) Chini, P. *J. Organomet. Chem.* **1980**, 200, 37.

(6) Zacchini, S. *Eur. J. Inorg. Chem.* **2011**, 4125.

(7) (a) Adams, R. D.; Trufan, E. *Philos. Trans. R. Soc. A* **2010**, 368, 1473. (b) Johnson, B. F. G.; Reynor, S. A.; Brown, D. B.; Shephard, D. S.; Mashmeyer, T.; Thomas, J. M.; Hermans, S.; Raja, R.; Sankar, G. *J. Mol. Catal. A* **2002**, 182–183, 89.

(8) (a) Shephard, D. S.; Maschmeyer, T.; Sankar, G.; Thomas, J. M.; Ozkaya, D.; Johnson, B. F. G.; Raja, R.; Oldroyd, R. D.; Bell, R. G. *Chem.—Eur. J.* **1998**, 4, 1214. (b) Adams, R. D.; Blom, D. A.; Captain, B.; Raja, R.; Thomas, J. M.; Trufan, E. *Langmuir* **2008**, 24, 9223. (c) Jones, M. D.; Duer, M. J.; Hermans, S.; Khimiyak, Y. Z.; Johnson, B. F. G.; Thomas, J. M. *Angew. Chem., Int. Ed.* **2002**, 41, 4726.

(9) (a) Albonetti, S.; Bonelli, R.; Epoupa Mengou, J.; Femoni, C.; Tiozzo, C.; Zacchini, S.; Trifirò, F. *Catal. Today* **2008**, 137, 483. (b) Albonetti, S.; Bonelli, R.; Delaigle, R.; Femoni, C.; Gaigneaux, E. M.; Morandi, V.; Ortolani, L.; Tiozzo, C.; Zacchini, S.; Trifirò, F. *Appl. Catal., A* **2010**, 372, 138. (c) Bonelli, R.; Albonetti, S.; Morandi, V.; Ortolani, L.; Riccobene, P. M.; Scirè, S.; Zacchini, S. *Appl. Catal., A* **2011**, 395, 10. (d) Bonelli, R.; Lucarelli, C.; Pasini, T.; Liotta, L. F.; Zacchini, S.; Albonetti, S. *Appl. Catal., A* **2011**, 400, 54. (e) Bonelli, R.; Zacchini, S.; Albonetti, S. *Catalysts* **2012**, 2, 1.

(10) (a) Schweyer-Tihay, F.; Estournès, C.; Braunstein, P.; Guille, J.; Paillaud, J. L.; Richard-Plouet, M.; Rosé, J. *Phys. Chem. Chem. Phys.* **2006**, 8, 4018. (b) Schweyer, F.; Braunstein, P.; Estournès, C.; Guille, J.; Kessler, H.; Paillaud, J. L.; Rosé, J. *Chem. Commun.* **2000**, 1271. (c) Schweyer-Tihay, F.; Braunstein, P.; Estournès, C.; Guille, J. L.; Lebeau, B.; Paillaud, J. L.; Richard-Plouet, M.; Rosé, J. *Chem. Mater.* **2003**, 15, 57.

(11) Robinson, I.; Zacchini, S.; Tung, L. D.; Maenosono, S.; Thanh, N. T. K. *Chem. Mater.* **2009**, 21, 3021.

(12) Rutledge, R. D.; Morris, W. H.; Wellons, M. S.; Gai, Z.; Shen, J.; Bentley, J.; Wittig, J. E.; Lukehart, C. M. *J. Am. Chem. Soc.* **2006**, 128, 14210.

(13) (a) Adams, R. D.; Cotton, F. A., Eds. *Catalysis by Di- and Polynuclear Metal Cluster Complexes*; Wiley-VCH: New York, 1998. (b) Braunstein, P.; Oro, L. A.; Raithby, P. R., Eds. *Metal Clusters in Chemistry*; Wiley-VCH: New York, 1999.

(14) Femoni, C.; Iapalucci, M. C.; Kaswalder, F.; Longoni, G.; Zacchini, S. *Coord. Chem. Rev.* **2006**, 250, 1580.

(15) (a) Longoni, G.; Iapalucci, M. C. In *Clusters and Colloids*; Schmid, G., Ed.; Wiley-VCH: New York, 1994; p 91. (b) Fumagalli, A.; Della Pergola, R. In *Metal Clusters in Chemistry*; Braunstein, P.; Oro, L. A.; Raithby, P. R., Eds.; Wiley-VCH: New York, 1999; p 323. (c) Lewis, J.; Raithby, P. R. In *Metal Clusters in Chemistry*; Braunstein, P.; Oro, L. A.; Raithby, P. R., Eds.; Wiley-VCH: New York, 1999; p 348.

(16) (a) Johnson, B. F. G.; Martin, C. M. In *Metal Clusters in Chemistry*; Braunstein, P.; Oro, L. A.; Raithby, P. R., Eds.; Wiley-VCH: New York, 1999; p 877. (b) Longoni, G.; Femoni, C.; Iapalucci, M. C.; Zanello, P. In *Metal Clusters in Chemistry*; Braunstein, P.; Oro, L. A.; Raithby, P. R., Eds.; Wiley-VCH: New York, 1999; p 1137.

(17) Femoni, C.; Iapalucci, M. C.; Longoni, G.; Wolowska, J.; Zacchini, S.; Zanello, P.; Fedi, S.; Riccò, M.; Pontiroli, D.; Mazzani, M. *J. Am. Chem. Soc.* **2010**, 132, 2919.

(18) Femoni, C.; Iapalucci, M. C.; Longoni, G.; Zacchini, S. *Eur. J. Inorg. Chem.* **2009**, 2487.

(19) Bernardi, A.; Femoni, C.; Iapalucci, M. C.; Longoni, G.; Ranuzzi, F.; Zacchini, S.; Zanello, P.; Fedi, S. *Chem.—Eur. J.* **2008**, 14, 1924.

(20) Bernardi, A.; Femoni, C.; Iapalucci, M. C.; Longoni, G.; Zacchini, S. *Dalton Trans.* **2009**, 4245.

(21) Collini, D.; Fabrizi de Biani, F.; Dolznikov, D. S.; Femoni, C.; Iapalucci, M. C.; Longoni, G.; Tiozzo, C.; Zacchini, S.; Zanello, P. *Inorg. Chem.* **2011**, 50, 2790.

(22) Femoni, C.; Iapalucci, M. C.; Longoni, G.; Zacchini, S.; Fedi, S.; Fabrizi de Biani, F. *Eur. J. Inorg. Chem.* **2012**, 2243.

(23) Femoni, C.; Iapalucci, M. C.; Longoni, G.; Zacchini, S.; Fedi, S.; Fabrizi de Biani, F. *Dalton Trans.* **2012**, 41, 4649.

(24) Bernardi, A.; Femoni, C.; Iapalucci, M. C.; Longoni, G.; Zacchini, S.; Fedi, S.; Zanello, P. *Eur. J. Inorg. Chem.* **2010**, 4831.

(25) Ciabatti, L.; Femoni, C.; Iapalucci, M. C.; Longoni, G.; Zacchini, S.; Zarra, S. *Nanoscale*, DOI: 10.1039/C2NR30400G.

(26) (a) Cordero, B.; Gómez, V.; Platero-Prats, A. E.; Revés, M.; Echevarria, J.; Cremades, E.; Barragán, F.; Alvarez, S. *Dalton Trans.* **2010**, 2832. (b) Bondi, A. *J. Phys. Chem.* **1964**, 68, 441.

(27) (a) Chini, P. *Chem. Commun.* **1967**, 440–441. (b) Albano, V.; Chini, P.; Scatturin, V. *Chem. Commun.* **1968**, 163–164.

(28) (a) Calderoni, F.; Demartin, F.; Fabrizi de Biani, F.; Femoni, C.; Iapalucci, M. C.; Longoni, G.; Zanello, P. *Eur. J. Inorg. Chem.* **1999**, 663. (b) Calderoni, F.; Demartin, F.; Iapalucci, M. C.; Longoni, G. *Angew. Chem., Int. Ed. Engl.* **1996**, 35, 2225. (c) Ceriotti, A.; Fait, A.; Longoni, G.; Piro, G.; Demartin, F.; Manassero, M.; Sansoni, M. *J. Am. Chem. Soc.* **1986**, 108, 8091.

(29) Mealli, C.; Proserpio, D. M. *J. Chem. Educ.* **1990**, 66, 399.

(30) Ceriotti, A.; Longoni, G.; Manassero, M.; Masciocchi, N.; Resconi, L.; Sansoni, M. *Chem. Commun.* **1985**, 181.

(31) (a) King, R. B. *New J. Chem.* **1988**, 12, 493. (b) Halet, J. F.; Evans, D. G.; Mingos, D. M. P. *J. Am. Chem. Soc.* **1988**, 110, 87.

(32) (a) Hughes, K.; Wade, K. *Coord. Chem. Rev.* **2000**, 197, 191. (b) Sironi, A. *Dalton Trans.* **1993**, 173.

(33) (a) Masters, A. F.; Meyer, J. T. *Polyhedron* **1995**, 14, 339.

(b) Battie, J. K.; Masters, A. F.; Meyer, J. T. *Polyhedron* **1995**, 14, 829.

(34) Femoni, C.; Iapalucci, M. C.; Longoni, G.; Zacchini, S. *Chem. Commun.* **2008**, 3157.

(35) (a) Ercoli, R.; Santambrogio, E.; Casagrande, G. T. *Chim. Ind. (Milan, Italy)* **1962**, 44, 1344–1349. (b) Dent, W. T.; Duncanson, L. A.; Guy, R. G.; Reed, H. W. R.; Shaw, B. L. *Chem. Ind.* **1961**, 169–170.

(36) Keller, E. *SCHAKAL99*; University of Freiburg: Germany, 1999.

(37) Sheldrick, G. M. *SADABS, Program for Empirical Absorption Correction*; University of Göttingen: Germany, 1996.

(38) Sheldrick, G. M. *SHELX97, Program for Crystal Structure Determination*; University of Göttingen: Germany, 1997.